



HAL
open science

Effect of an electric field on a floating lipid bilayer: A neutron reflectivity study

S. Lecuyer, G. Fragneto, Thierry Charitat

► **To cite this version:**

S. Lecuyer, G. Fragneto, Thierry Charitat. Effect of an electric field on a floating lipid bilayer: A neutron reflectivity study. *European Physical Journal E: Soft matter and biological physics*, 2006, 21 (2), pp.153-159. 10.1140/epje/i2006-10054-8 . hal-02301224

HAL Id: hal-02301224

<https://hal.science/hal-02301224>

Submitted on 17 Nov 2021

HAL is a multi-disciplinary open access archive for the deposit and dissemination of scientific research documents, whether they are published or not. The documents may come from teaching and research institutions in France or abroad, or from public or private research centers.

L'archive ouverte pluridisciplinaire **HAL**, est destinée au dépôt et à la diffusion de documents scientifiques de niveau recherche, publiés ou non, émanant des établissements d'enseignement et de recherche français ou étrangers, des laboratoires publics ou privés.

Effect of an electric field on a floating lipid bilayer: a neutron reflectivity study

Sigolène Lecuyer and Thierry Charitat
*Institut Charles Sadron, UPR 22, CNRS-Université Louis Pasteur,
6 rue Boussingault, F-67083 Strasbourg Cedex, France*

Giovanna Fragneto
Institut Laue-Langevin, 6 rue Jules Horowitz, B.P. 156, 38042 Grenoble Cedex, France

We present here a neutron reflectivity study of the influence of an alternative electric field on a supported phospholipid double bilayer. We report for the first time a reproducible increase of the fluctuation amplitude leading to the complete unbinding of the floating bilayer. Results are in good agreement with a semi-quantitative interpretation in terms of negative electrostatic surface tension.

PACS numbers: 87.16.Dg, 87.15.Va, 61.12.Ha

I. INTRODUCTION

In an aqueous environment, phospholipids self-assemble into bilayers; these 2D systems have been recently extensively studied, as they display complex peculiar behaviours [1, 2], and constitute the major component of the cell membrane [3]. The strong influence of electric fields on lipid bilayers is interesting both from a fundamental point of view and for practical aspects, and has consequently received an important research effort. Large electric fields are also used to introduce macromolecules in vesicles or cells by formation of long-lived pores in the bilayer [4, 5], and also by endocytosis [6]. Smaller alternative electric fields are commonly used to destabilise lipid bilayers in order to form large unilamellar vesicles [7, 8] in the so called *electroformation* technique. Recently Burgess et al. [9] have studied the effect of a static electric field (surface charge) on the structure of supported bilayers.

Although it is a widely used technique, the mechanism involved in vesicle electroformation is not well understood yet. In a recent theoretical paper [10], Sens and Isambert have suggested that a "negative surface tension" due to the electric field induces an undulation instability of the bilayer, and that hydrodynamical effects select the fastest-destabilised mode. These predictions are difficult to test in classical electroformation experiments. As a matter of fact, the initial system is usually a rather disordered lamellar phase, obtained by hydration of a dry lipid film and, consequently, the result is very polydisperse in both size and degree of lamellar order. Recently, Constantin et al. [11] have reported the first study of membrane destabilisation by an electric field on a more controlled system: a solid-supported fully-hydrated oriented lamellar phase (from 10 to 3000 bilayers). They observed for the first time individual peeling of the bilayers, but were not able to confirm or refute the existence of electrodynamical instability.

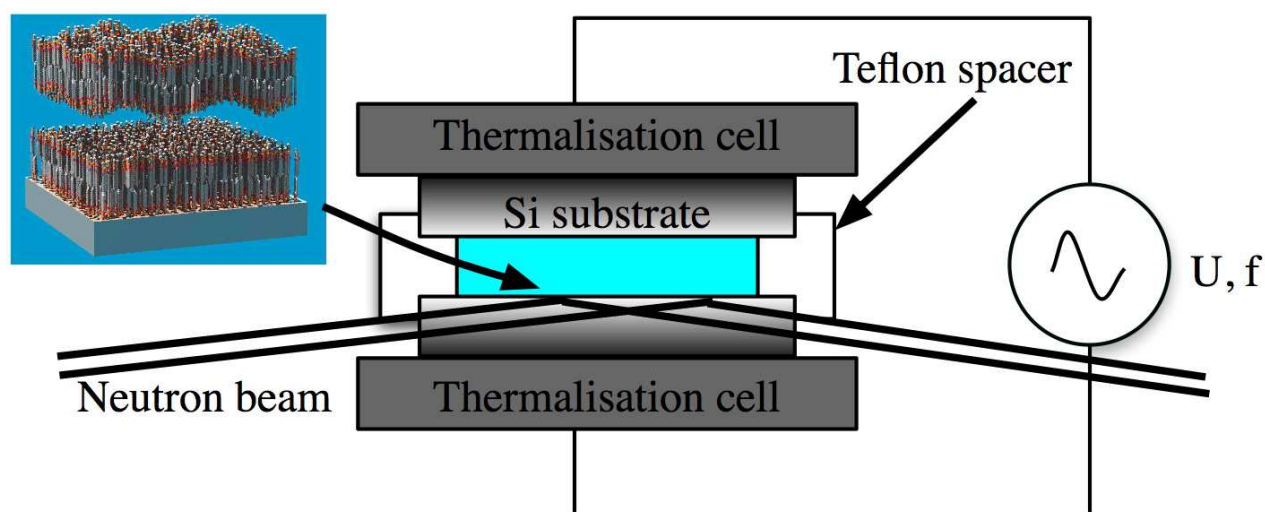


FIG. 1: Experimental set-up: the two identical silicon substrates (10 mm-thick) are in thermal and electrical contact with thermalisation blocks. The PTFE spacer ensures a 5 mm separation between the two blocks.

Because they are quite free of defects, double-bilayer systems are promising candidates to reach better understanding of the mechanism of vesicle formation in a well-defined geometry. Recent work has shown that they enable local study of the destabilisation of a single membrane [12]. In this paper we focus on the first steps of the bilayer destabilisation by an electric field as detected by neutron reflectivity.

II. MATERIALS AND METHODS

A. Sample preparation

Supported single and double-bilayers of DPPC and DSPC (1, 2-dipalmitoyl-sn-glycero-3-phosphocholine and 1, 2-distearoyl-sn-glycero-3-phosphocholine, Avanti Polar Lipids) molecules were prepared using the Langmuir-Blodgett and Langmuir-Schaefer techniques, as described in detail previously [13].

Bilayers were deposited on silicon substrates (highly doped 2-10 $\Omega\cdot\text{cm}^{-1}$, $5\times 5\times 1\text{ cm}^3$), polished to produce a high quality crystal surface with r.m.s. roughness $< 0.2\text{ nm}$ (SILTRONIX, Archamps, F). After careful cleaning, the silicon blocks were made highly hydrophilic by a UV/ozone treatment as in [13]. Lipid depositions were performed at a constant surface pressure of 40 mN/m, the Langmuir trough (NIMA, Warwick, UK) being thermalised at 20°C. Transfer ratios for the first layers were always high and of the same order as for samples described in [13]. A very precise adjustment of sample horizontality during the Schaefer dip, crucial for a good quality sample, led to transfer ratios always bigger than 0.96. After the deposition of the fourth layer, samples were constantly kept into water. They were closed while submerged in the trough, using a 5 mm-thick-PTFE spacer and a similar silicon substrate as a lid, and then placed into a water-regulated temperature chamber (see figure I).

Annealing was generally performed by progressively heating the sample to the fluid phase and then cooling it back to the gel phase. Then after careful characterisation of the structure in the gel and the fluid phases, the adopted protocol consisted in applying to the supported fluid bilayer(s) an alternative electric field of fixed amplitude, decreasing gradually the frequency (from 200 Hz to 5 Hz). For each value of the frequency reflectivity data were collected. All measurements were made at 62°C to ensure sample fluidity.

B. Neutron reflectivity: basic principles and measurements

Specular reflectivity, $R(q)$, defined as the ratio between the specularly reflected and incoming intensities of a neutron beam, is measured as a function of the wave vector transfer, $q = 4\pi \sin\theta/\lambda$ perpendicular to the reflecting surface, where θ is the angle and λ the wavelength of the incoming beam. $R(q)$ is related to the scattering length density across the interface, $\rho(z)$, by the relation [14]:

$$R(q) = \frac{16\pi^2}{q^2} |\tilde{\rho}(q)|^2 \quad (1)$$

where $|\tilde{\rho}(q)|$ is the one-dimensional Fourier Transform of $\rho(z)$.

Specular reflectivity allows the determination of the structure of matter perpendicular to a surface or an interface. Experiments are performed in reflection at grazing incidence. Samples must be planar, very flat and with roughness as small as possible. Data were collected at the High Flux Reactor (HFR) of the Institut-Laue Langevin (ILL, Grenoble, F) both on the small angle diffractometer D16 (preliminary measurements) and on the high flux reflectometer D17, designed to take advantage of both Time-Of-Flight (TOF) and monochromatic methods of measuring reflectivity (dual mode instrument) [15, 16]. In this study measurements were all taken with the instrument in the TOF mode by using a spread of wavelengths between 2 and 20 Å at two incoming angles (typically 0.7° and 4°) and with a resolution, defined by two choppers, of $\Delta t/t = 1\%$ and 5%, respectively, where Δt is the neutron pulse duration. The beam was defined in the horizontal direction by a set of two slits, one just before the sample and one before a vertically focusing guide. Neutron reflectivity from the same sample was measured at different temperatures monitored with a thermocouple (equilibration time 25 minutes, stability $< 0.1^\circ\text{C}$, absolute precision $< 0.3^\circ\text{C}$), in the water-regulated sample chamber already described in [13]. The useful q -range, before hitting the sample background, spanned from 0.007 to 0.24 \AA^{-1} and was measured in about two hours, also after equilibration. The equilibration time varied depending on the step of temperature increase or decrease. For a step of 1°C it was of about 15 minutes.

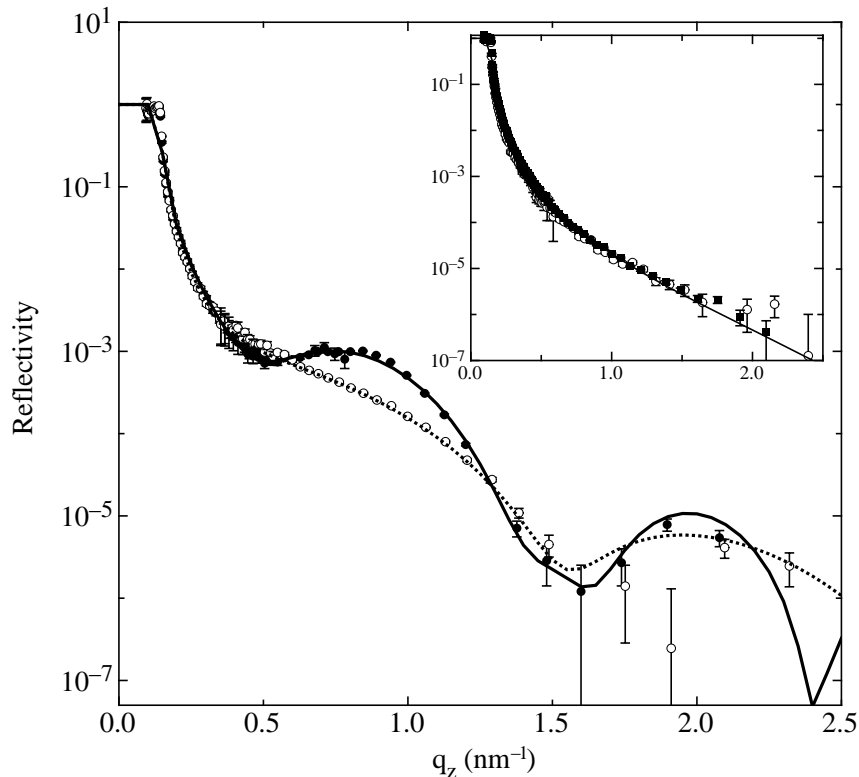


FIG. 2: Reflectivity curves: closed circles (●) = double DSPC bilayer in CaCl_2 before applying electric field and best fit with a double bilayer model (full line); open circles (○) = after applying a (10 V, 10 Hz) field and best fit with a single bilayer model (dashed line). In insert, reflectivity curves for the bare substrate before and after the experiment (and best fit with a silicon oxide layer model).

C. Analysis of reflectivity data

Specular reflectivity is a technique able to resolve the stacking of several slabs each one with a certain thickness and a certain scattering length density. Data analysis requires a good knowledge of the sample and here it was done via model fitting. Born and Wolf gave a general solution, the so called optical matrix method [17], to calculate the reflectivity from any number of parallel, homogeneous layers, which is particularly useful since any layered structure can be approximately described by dividing it into an arbitrary number of layers parallel to the interface, each having a uniform scattering length density. A reflectivity curve essentially reflects the sample density perpendicular to the substrate surface, or rather the square modulus of its Fourier transform. Since the phase is lost, data need to be fitted (e.g. with a slab model) to extract the density profile. In previous studies [13], multiple contrast neutron measurements have determined within Å precision the profile of adsorbed and floating bilayers, in the gel and the fluid phases. Each bilayer is resolved into outer-inner-outer slabs: outer slabs = heads (phosphocholine and glycerol groups), inner slab = tails (hydrocarbon chains). A water film of thickness D_w separates the adsorbed and floating bilayers. Taking into account the water layer between the adsorbed bilayer and the substrate and the silicon oxide layer, this leads to 9 slabs in total, each one having its own average thickness and scattering length density. Moreover, each interface between two slabs has a certain width, also called r.m.s. roughness. Since this enters into the density profile, it can be determined by fits of reflectivity curves, but it is not possible to determine whether it is a static intrinsic width or an average over the neutron beam's correlation length of temporal or spatial fluctuations.

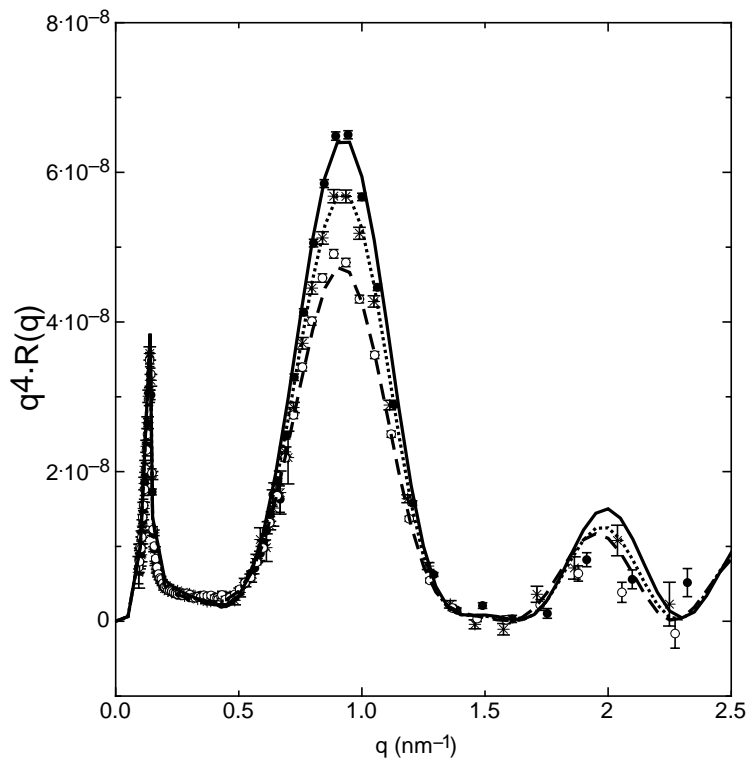


FIG. 3: Modification of the reflectivity curve with respect to the frequency of the electric field. A 5V alternative field is applied to a DSPC double bilayer in D_2O ; full circles (\bullet) with $f=100$ Hz; stars (\star) with $f=50$ Hz; open circles (\circ) with $f=10$ Hz. The lines are the best fits obtained with the values of the roughness given in the text.

III. RESULTS

A. Complete unbinding in a highly conductive solution

The first result of this paper is the observation for the first time of the floating bilayer complete unbinding by application of an electric field. This effect was observed on two different samples under the same conditions: double bilayers of DSPC in a $CaCl_2$ in D_2O solution (0.35 mM.l^{-1} , measured conductivity of $16.62 \mu\text{S.cm}^{-1}$) at low frequency (10 Hz) and for a voltage amplitude higher than 5 V. Figure 2 shows reflectivity data for one of these double bilayer DSPC samples before and after applying the electric field. The curves correspond to the best fits obtained with a 9-slab model and are in good agreement with previous multi-contrast neutron reflectivity experiments [13].

After the unbinding we still observed the presence of the first bilayer, without any major change in structure, but slightly shifted away from the substrate (figure 2). After removing the bilayer by cleaning the substrate we could confirm that the silicon oxide layer was unmodified and therefore that there was no formation of porous silicon oxide (figure 2 in insert). The adsorbed bilayer might possibly be removed by application of a lower frequency or/and higher voltage field, but this could not be tested as it could have induced significant oxidation of the silicon. As a matter of fact, we had previously been able to determine that the formation of porous silicon oxide is very sudden and occurs when frequency becomes lower than 5 Hz in identical conditions (unpublished data).

B. Progressive increase of fluctuations in a poorly conductive solution

1. Double bilayer

As this complete unbinding of the floating bilayer is very sudden, we tried to observe previous steps of the destabilisation in a low conductivity electrolyte such as D_2O ($\chi_s^{-1} = 0.34 \mu\text{S.cm}^{-1}$). We performed experiments on a DSPC double bilayer in these conditions, and were able to observe a progressive modification of the reflectivity curves (figure 3).

- At high frequencies ($f > 100$ Hz), this modification appeared to be irreversible and involved mainly the first bilayer: the thin water layer (~ 0.3 nm, see table I) initially separating the substrate and the first bilayer disappears (or becomes smaller than our experimental resolution), while the amount of solvent in the bilayer increases from 2% to 6%. For this first confined bilayer, assuming that the first water layer behaves as a dielectric, both effects could originate from the electrostatic pressure acting on the effective silicon oxide-water layer-bilayer capacitance. Note that at the same time the second bilayer structure is unmodified.
- At lower frequencies, modifications also involved the floating bilayer roughness and were partially reversible. It is very difficult to determine which structural parameter(s) is/are responsible for the subtle modifications observed without additional information. Nevertheless, as previously mentioned no modification of the silicon oxide layer was detected. The structure of the double bilayer can be well determined before applying the electric field [13], and the global structure of the bilayers (i.e. the slabs number and nature) seems to be unaffected by the electric field. It thus seemed physically reasonable to fit the reflectivity curves under electric field by varying mainly bilayers roughness and water layers thickness; average percentages of solvent within the bilayers were also allowed to vary, accounting for the induced formation of defects or pores in the membranes.

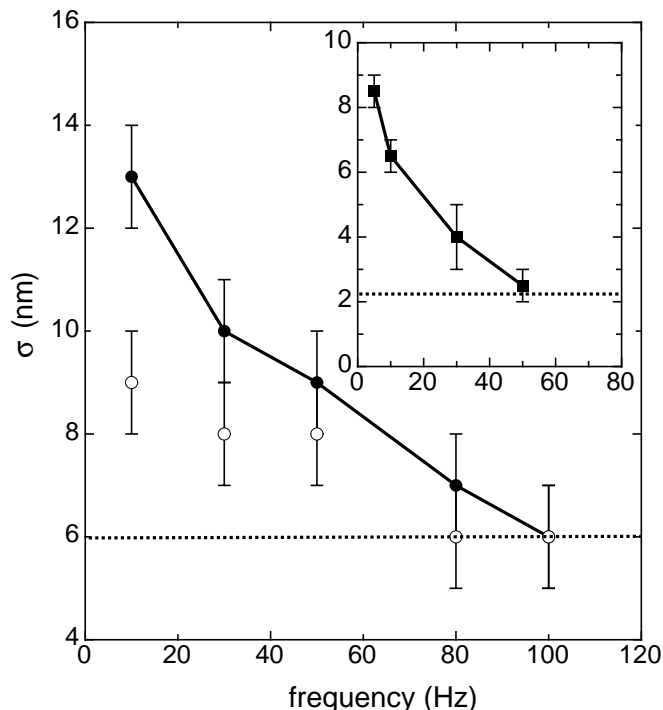


FIG. 4: Top bilayer roughness vs electric field frequency f at constant field amplitude $V_{pp}/2 = 5V$: (●) DSPC double-bilayer in D_2O (in insert, (■) same curve for a DSPC bilayer); (○) reversibility test after each frequency (no electric field) for the double bilayer.

Within this framework, the dominant effect we observed was a progressive increase of the floating (top) bilayer roughness, going from 0.6 ± 1 to 1.3 ± 1 nm. Again it was not possible to go to lower frequencies or higher voltages to avoid substrate deterioration, and in the frequency-range studied no complete unbinding occurred in D_2O .

This roughness increase seemed to be partially reversible, as shown on figure 4. Reversibility was systematically checked in the low conductivity solution (D_2O); for beam time limitation reasons we were not able to check it in the $CaCl_2$ conductive solution. A small increase of the thickness of water between the bilayers $D_{w,2}$, in the limit of the resolution of the experiment, was also observed. Finally, a progressive increase of the percentage of solvent in the first, substrate-bound bilayer was also observed, while the percentage of solvent in the floating bilayer remained constant and very low. Whether this corresponds to the formation of pores - made easier by the higher tension of the supported membrane, or of permanent holes due to electrochemical phenomena close to the substrate is unsure. However the latter seems more likely as this increase of the solvent content was apparently not reversible.

The irreversible effect on the first bilayer at frequencies > 100 Hz, as well as the reversible effect at low frequencies, well described by an increase of the top bilayer roughness, were observed on different DSPC samples. Nevertheless, as we were not able to check carefully the stability of the oxide layer in these cases we do not report corresponding data in the present paper.

2. Single bilayer

In order to check the effect of the electric field on the first, substrate-bound bilayer, we performed experiments on a single supported DSPC bilayer. Results are shown in figure 4 (insert). They showed a progressive increase of the bilayer roughness, along with an increase of membrane-substrate distance. However no modification of the bilayer structure was seen, and the percentage of solvent remained very low ($\sim 2\%$), in agreement with a good-quality sample. We can thus think that, in the case of the double-bilayer, the solvent increase in the first bilayer is correlated to the fact that it is confined close to the substrate by the second, fluctuating bilayer. This seems consistent with the fact that when the second bilayer unbinds, the first one relaxes away from the substrate.

IV. DISCUSSION

The results reported above clearly show that an electric field can induce a complete destabilisation of the top bilayer of a double-bilayer at low frequency (~ 5 -10 Hz). This very abrupt destabilisation follows a reversible increase of the bilayer roughness. It is tempting to describe this roughness in terms of thermal fluctuations, and we intend to do so in this section.

A. Bilayer fluctuations

We consider the small thermal fluctuations of a single bilayer close to a substrate. Using common notations (see [18] for example), we note $\vec{r} = (x, y)$ the in plane coordinates and z the coordinate normal to the substrate and we call $u(\vec{r}) = u(x, y)$ the membrane position. Classical Helfrich's Hamiltonian [19] can then be written at first order expansion in membrane's curvature as :

$$\mathcal{H}[u(\vec{r})] = \int_S d^2\vec{r} \left[U(u(\vec{r})) + \frac{1}{2}\kappa(\Delta u(\vec{r}))^2 + \gamma(\vec{\nabla}u(\vec{r}))^2 \right]. \quad (2)$$

where κ is the bending modulus of the bilayer, γ its surface tension and U the membrane-substrate interaction potential. Using a quadratic approximation for $U(u(\vec{r}))$ it is possible to apply the equipartition theorem for small fluctuations:

$$\langle |u_q|^2 \rangle = \frac{1}{S} \times \frac{k_B T}{U'' + \gamma q^2 + \kappa q^4} \quad (3)$$

Note that this expression is only valid when the fluctuation amplitude is smaller than the mean distance to the substrate, which seems to be the case in our experiments. For large fluctuations one would have to take into account the reduction of entropy caused by the substrate, leading to the so-called Helfrich repulsion [2, 18].

In their recent paper, Sens and Isambert [10] describe the case of a free membrane far from a substrate ($U'' = 0$) and take into account the effect of hydrodynamics on the bilayer destabilisation. In particular, they showed that energy dissipation by solvent flow (viscosity η) and by monolayer-monolayer friction (friction coefficient b_{fr}) lead to the selection of a fastest-destabilised mode of wavelength q^* :

$$q^* = \frac{(\Gamma_{el} - \gamma)\eta}{\kappa b_{fr} \delta^2} \simeq 1 \mu m^{-1} \quad (4)$$

This length scale is in good agreement with the characteristic size of vesicles prepared by electroformation.

In our experimental study, the two bilayers are not free but interact with the substrate and the other bilayer. Bilayer equilibrium position without electric field is thus given by a competition between hydration repulsive forces and van der Waals attractive ones, as described in ref.[2, 18].

Using Eq. 3, it is possible to calculate the rms amplitude of fluctuations σ^2 :

$$\begin{aligned}\sigma^2 &= \langle z(r)^2 \rangle = \frac{1}{(2\pi)^2} \int d^2\vec{q} \langle |u_q|^2 \rangle \\ &= \frac{k_B T}{2\pi\sqrt{\Delta}} \log \frac{q_2}{q_1}\end{aligned}\quad (5)$$

with $\Delta = \gamma^2 - 4U''\kappa$, $q_1^2 = \frac{\gamma - \sqrt{\Delta}}{2\kappa}$ and $q_2^2 = \frac{\gamma + \sqrt{\Delta}}{2\kappa}$.

At the linear order, the effect of an electric field on the membrane can be expressed as a negative surface tension $-\Gamma_{el}$ (with $\Gamma_{el} > 0$). Following the notations of ref. [10], Γ_{el} can be written as:

$$\Gamma_{el} = \epsilon_m E_m^2 \delta \quad (6)$$

where ϵ_m is the membrane dielectric constant, E_m is the local electric field and δ the bilayer thickness. This negative surface tension induces enhanced thermal fluctuations that can be described by replacing γ by $\tilde{\gamma} = \gamma - \Gamma_{el}$ in equation 3. Figure 5 shows the variation of σ as a function of the global surface tension $\gamma - \Gamma_{el}$; here we have taken $\kappa \simeq 40k_B T$ and $U'' \simeq 10^{13} \text{ J.m}^{-4}$, which are classical values for a DSPC bilayer in the fluid phase [20].

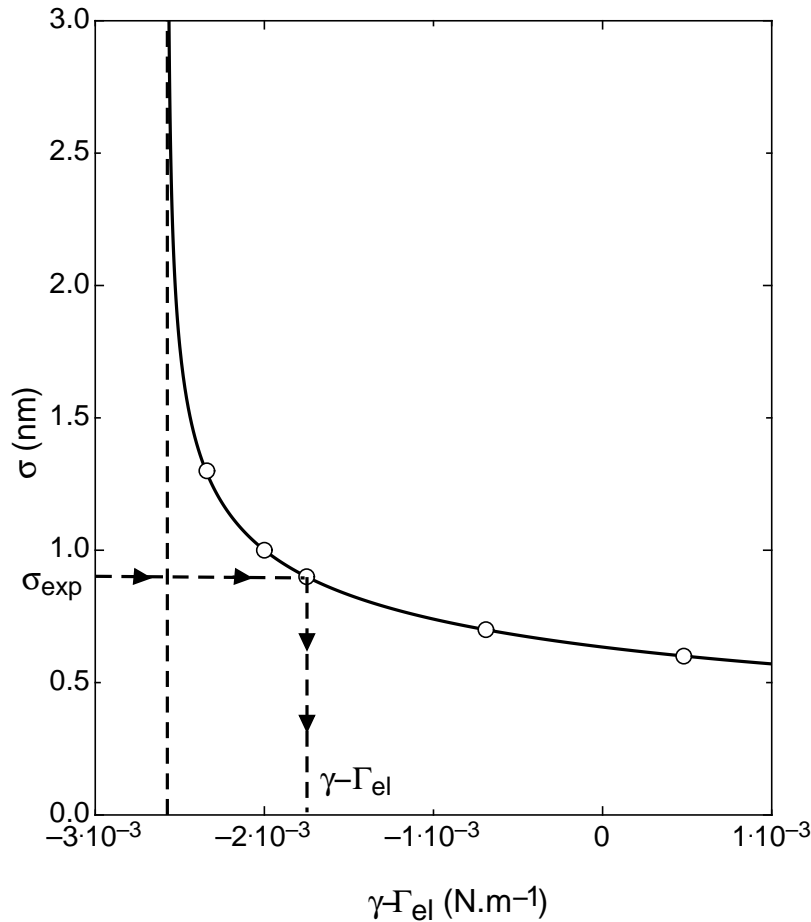


FIG. 5: Membrane rms fluctuation amplitude σ as a function of global surface tension $\gamma - \Gamma_{el}$, deduced from equation 5. (o): values probed during the experiments.

Membrane fluctuations undergo a sharp divergence for a finite negative value of $\tilde{\gamma}_c = -\sqrt{U''\kappa}$ which is the signature of bilayer destabilisation. This unbinding occurs in a very narrow surface tension range, which could explain the abrupt destabilisation observed in our experiments.

B. Discussion in terms of electrostatic surface tension

Let us now try to evaluate the electric surface tension equivalent to the field we have applied. It is possible to derive values of Γ_{el} using equation 5, if we know σ , γ , κ and U'' . We measured σ experimentally. Previous X-ray off-specular experiments [20] have shown on very similar samples (a fluid DSPC bilayer deposited on an hybrid OTS-DSPC bilayer) that $\kappa \simeq 40 k_B T$ and $\gamma \simeq 0.5 \text{ mN.m}^{-1}$. Using these experimental results we can fix U'' to obtain the correct experimental value of σ measured without any electric field. Following this method we obtain $U'' \simeq 10^{13} \text{ J.m}^{-4}$. This value is in good agreement with theoretical estimations using a van der Waals potential [2]. It is then possible by using equation 5 to derive numerical values of Γ_{el} for the different fields applied, which are reported on figure 5.

Following ref. [10], the electrostatic surface tension Γ_{el} (Eq. 6) can be related to the electric field E applied to the whole cell by:

$$\Gamma_{el} \simeq \epsilon_m \left(\frac{\chi_m}{\chi_s} \right)^2 E^2 \delta \quad (7)$$

where χ_m^{-1} and χ_s^{-1} are respectively the membrane and solvent conductivity. With $\epsilon_m \simeq 2\epsilon_0$, $\chi_s^{-1} = 0.34 \times 10^{-4} \text{ S.m}^{-1}$ for D_2O (measured experimental value) and $\Gamma_{el} \sim 10^{-3} \text{ N.m}^{-1}$ it leads to $\chi_m^{-1} \sim 3 \times 10^{-10} \text{ S.m}^{-1}$ (equivalent to a membrane resistance $R_m \sim 0.2 \text{ M}\Omega.\text{cm}^2$), in good agreement with the value obtained by Purrucker et al. [21]. In the high conductivity solution (CaCl_2 , $\chi_s^{-1} = 16 \times 10^{-4} \text{ S.m}^{-1}$), even if we found no value of the membrane conductivity reported in literature, it seems clear that we are well above the unbinding surface tension γ_c .

Field frequency seems to be an important parameter in membrane destabilisation. We were not able to detect any modification (reversible or irreversible) of the bilayer above 100 Hz whereas the effect becomes important below 10 Hz (Fig. 4 and 7). This is in good agreement with previous observations by Constantin et al. [11]. It is also precisely the frequency range used in electroformation techniques. In order to understand more quantitatively this effect, let us try to estimate the local electric field acting on the bilayer. We can do so by using a simple equivalent circuit to represent the experimental set-up (figure 6).

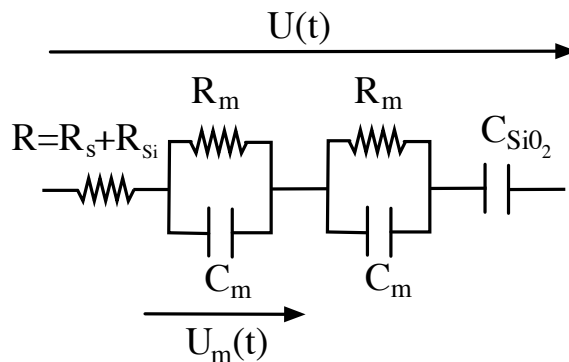


FIG. 6: A simple equivalent circuit for the system.

The bilayer impedance Z_m is modelled by a resistance R_m and a capacitance C_m in parallel [21]. The substrate is described by a resistance $R_{Si} (\ll 1\Omega)$ and a capacitance attributed to the silicon oxide $C_{SiO_2} (\simeq 30 \mu\text{F}$ for a 1 nm-thick oxide) in series. The electrolyte solution has a resistance $R_s (\simeq 92 \text{ k}\Omega$ for D_2O). It is then easy to derive the negative electrostatic surface tension acting on the bilayer:

$$\Gamma_{el} = \frac{1}{2} \epsilon_m \left(\frac{R_m}{R} \right)^2 \frac{U_0^2}{\delta} \frac{(\omega\tau_i)^2}{(1 - \omega^2\tau_m\tau_i)^2 + \omega^2(\tau_m + \tau_i(1 + n\beta))^2}$$

where n is the number of bilayer(s), R the total resistance $R = R_s + R_{Si}$, $\beta = \frac{R_m}{R}$ and we have introduced the two characteristic times $\tau_m = R_m C_m$ and $\tau_i = R C_{SiO_2}$.

Using $R_s = 92 \text{ k}\Omega$ and $C_{SiO_2} = 30 \mu\text{F}$ as fixed values, the best fit to the data gives $R_m = 48 \pm 1 \text{ k}\Omega$ ($\sim 0.78 \pm 0.2 \text{ M}\Omega.\text{cm}^2$) and $C_m = 0.1 \pm 0.01 \mu\text{F}$ ($\sim 0.01 \pm 0.005 \mu\text{F.cm}^{-2}$). The corresponding result is plotted figure 7. The value of R_m is in very good agreement with typical values of bilayer membranes resistance, around 0.9-1 $\text{M}\Omega.\text{cm}^2$ for a high coverage of the substrate (see for example Ref. [21, 22]). However the value of C_m is surprisingly lower than values

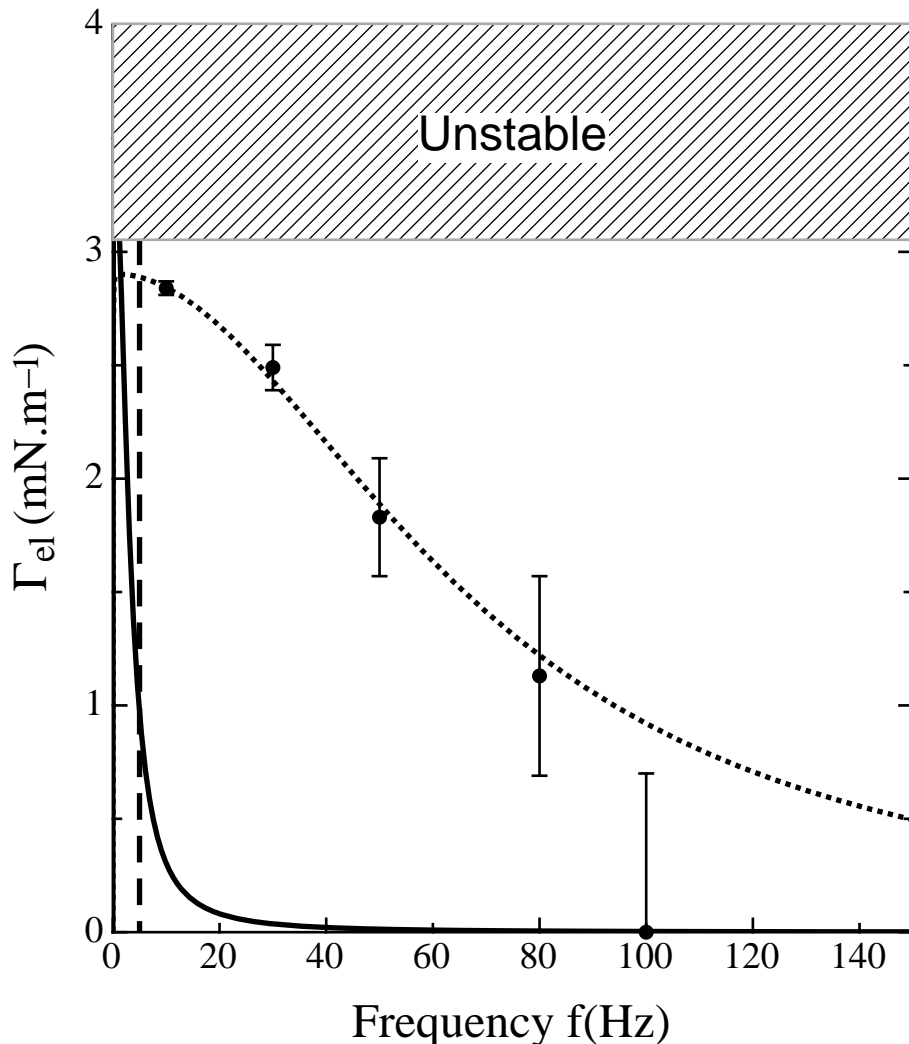


FIG. 7: Γ_{el} as a function of frequency: (•) values derived from experimental data; dashed line = best fit using equation 8; full line = equation 8 with $R_m = 60 \text{ k}\Omega$ and $C_m = 2\mu\text{F}$. We have represented by a dashed line the frequency limit ($f \sim 5 \text{ Hz}$) where silicon oxidation is observed.

usually found for supported bilayers ($\sim 0.5 \mu\text{F}\cdot\text{cm}^{-2}$ [21, 22]). We have no explanation for this disagreement. Many effects could account for it, including the fact that the first membrane might be damaged by the field. Maybe our model is then too simple to give a good description of the system capacitive behaviour. We have drawn on figure 7 the curve obtained with a more consistent value of the membrane capacitance. In any case, we can notice that the frequency behaviour we observe is similar to previous observations by Constantin and coworkers [11].

V. CONCLUSIONS AND PERSPECTIVES

In this work we have reported the effect of an alternative electric field on lipid double bilayers adsorbed on doped silicon substrates, as studied by neutron reflectivity. We clearly show that the electric field can lead to a complete unbinding of the floating bilayer in a high conductivity solution at low frequency. In a low conductivity solution, small reversible modifications of the reflectivity profiles are observed and described as changes of the rms roughness of the floating bilayer. These data could be interpreted with a fluctuation spectrum including a negative electrostatic surface tension term as suggested by ref. [10]. Electric field frequency seems to be an important parameter as no effect is observed above 100 Hz. This result is also consistent with previous observations [11]. We have tried to understand this effect with a simple electrokinetic model of the cell.

To the author's knowledge, this is the first time that the effect of an alternative electric field on the fluctuations of a membrane close to a wall is studied. We have clearly shown that it is possible to completely destabilise a single bilayer by using an electric field in a well defined geometry. This work should be useful in the future for a better understanding of phenomena such as vesicle electroformation.

However, so far our results provide no information on the lateral length scale (q^* in ref. [10]) of the instability, which is one of the main predictions of the theoretical model [10]. We only measure the integrated root-mean-square amplitude σ of fluctuations. In a near future, we plan to perform off-specular reflectivity experiments, as described in ref. [20]. They could provide important information concerning the lateral length scale(s) of the changes involved, and will enable direct measurement of the fluctuation spectrum and the surface tension.

Acknowledgments: The authors wish to thank Michel Bonnaud for technical assistance and the ILL for providing neutron beam-time.

TABLE I: Structural parameter of a DSPC double bilayer in D₂O before any electric field is applied: (sld) = scattering length densities in 10⁻⁶ Å⁻²; thicknesses and roughnesses in Å. All values are obtained from the best fit (figure 2).

	Silicon oxide	Solvent	Head	Chains	Head	Solvent	Head	Chains	Head
thickness	11 ± 1	3 ± 0.5	6 ± 1	36 ± 1	6 ± 1	19 ± 0.5	6 ± 1	36 ± 1	6 ± 1
sld	3.4 ± 0.1	0	2.05 ± 0.1	-0.6 ± 0.05	2.05 ± 0.1	0	2.05 ± 0.1	-0.6 ± 0.05	2.05 ± 0.1
% solvent	1 ± 1	100	19 ± 3	2 ± 1	19 ± 3	100	19 ± 3	2 ± 1	19 ± 3
roughness	3 ± 0.5	2 ± 1	3 ± 1	4 ± 1	3 ± 1	5 ± 1	3 ± 1	6 ± 1	3 ± 1

-
- [1] Katsaras, Gutberlet, *Lipid Bilayers*, Biological Physics Series (Springer, 2000)
 - [2] R. Lipowsky, *Handbook of Biological Physics, vol. 1* (Elsevier, 1995)
 - [3] O. Mouritsen, O. Andersen, eds., *In search of a new biomembrane model*, Vol. 49 (Copenhagen, 1998)
 - [4] J.C. Weaver, Y.A. Chizmadzhev, *Bioelectrochemistry and Bioenergetics* **41**, 135 (1996)
 - [5] H. Isambert, *Physical Review Letters* **80**, 3404 (1998), <http://link.aps.org/abstract/PRL/v80/p3404>
 - [6] Y. Rosemberg, R. Korenstein, *Bioelectrochemistry and Bioenergetics* **42**, 275 (1997)
 - [7] M.I. Angelova, D. Dimitrov, *Faraday Discussion* **81**, 303 (1986)
 - [8] M.I. Angelova, S. Soleau, P. Méléard, J.F. Faucon, P. Bothorel, *Progress in Colloid and Polymer Science* **89**, 127 (1992)
 - [9] I. Burgess, M. Li, S.L. Horswell, G. Szymanski, J. Lipkowski, J. Majewski, S. Satija, *Biophysical Journal* **86**, 1763 (2004)
 - [10] P. Sens, H. Isambert, *Physical Review Letters* **88**, 128102 (2002)
 - [11] D. Constantin, C. Ollinger, M. Vogel, T. Salditt, *The European Physical Journal E* (2005)
 - [12] S. Lecuyer, T. Charitat, *Europhysics Letters* **75**, 652 (2006)
 - [13] T. Charitat, E. Bellet-Amalric, G. Fragneto, F. Graner, *European Physical Journal B* **8**, 583 (1999)
 - [14] J. Penfold, R.K. Thomas, *Journal of Physics: Condensed Matter* **2**, 1369 (1990)
 - [15] R. Cubitt, G. Fragneto, *Neutron Reflection: Principles and Examples of Applications*, in *Scattering*, edited by R. Pike, P. Sabatier (Academic Press, London, 2002), pp. 1198–1208
 - [16] R. Cubitt, G. Fragneto, *Applied Physics A* **74**, 329 (2002)
 - [17] M. Born, E. Wolf, *Principles of Optics* (Pergamon Press, Oxford, 1989)
 - [18] K.R. Mecke, T. Charitat, F. Graner, *Langmuir* **19**, 2080 (2003)
 - [19] W. Helfrich, *Zeitschrift für Naturforschung* **28**, 693 (1973)
 - [20] J. Daillant, E. Bellet-Amalric, A. Braslau, T. Charitat, G. Fragneto, F. Graner, S. Mora, F. Rieutord, B. Stidder, *The Proceeding of the National Academy of Sciences USA* **102**, 11639 (2005)
 - [21] O. Purrucker, H. Hillebrandt, K. Adlkofer, M. Tanaka, *Electrochimica Acta* **47**, 791 (2001)
 - [22] V. Atanasov, N. Knorr, R.S. Duran, S. Ingebrandt, A. Offenhäusser, W. Knoll, I. Köper, *Biophysical Journal* **89**, 1780 (2005)